

# Enhanced nonlinear circular dichroism in resonant dielectric metasurfaces

Kirill Koshelev,<sup>†,‡</sup> Yutao Tang,<sup>¶</sup> Zixian Hu,<sup>¶</sup> Ivan Kravchenko,<sup>§</sup>

Guixin Li,<sup>¶</sup> and Yuri Kivshar<sup>\*,†,‡</sup>

<sup>†</sup>*Nonlinear Physics Center, Research School of Physics, Australian National University,  
Canberra ACT 2601, Australia*

<sup>‡</sup>*School of Physics and Engineering, ITMO University, St Petersburg 197101, Russia*

<sup>¶</sup>*Department of Material Science and Engineering, Shenzhen Institute for Quantum Science  
and Engineering, Southern University of Science and Technology, Shenzhen 518055, China*

<sup>§</sup>*Center for Nanophase Materials Sciences, Oak Ridge National Laboratory, Oak Ridge,  
Tennessee 37831, United States*

E-mail: yuri.kivshar@anu.edu.au

## Abstract

We study both linear and nonlinear circular dichroism in dielectric resonant metasurfaces. We predict and demonstrate experimentally the enhancement of circular dichroism for normal propagation of light due to the excitation of multipolar Mie-type modes in silicon resonators and the formation of a complex vectorial field structure. We also reveal that high-quality Mie resonances satisfying optimal coupling condition can lead to giant circular dichroism in the nonlinear regime observed for the generation of the third-harmonic signal by normally propagating circularly polarized fundamental frequency fields.

## Keywords

dielectric metasurfaces, chirality, Mie resonances, third-harmonic generation

## Introduction

Chiral structures represent a class of systems that cannot be superimposed with themselves after mirror reflection. This property finds many useful applications in nanophotonic structures made of chiral elements which can exhibit chiroptical effects such as circular dichroism (CD) for left and right circularly polarized excitation.<sup>1</sup> Over the last decade a number of demonstrations of strong chiroptical effects was done in planar dielectric and plasmonic metastructures,<sup>2-6</sup> which lack fabrication complexity of bulky three-dimensional metamaterials. In particular, it was shown that planar structures supporting pronounced resonances can exhibit strong nonreciprocal CD via mode interference despite a lower chiroptical response imposed by inherent reflection symmetry.<sup>7</sup> Recently, it was shown that chiral dielectric metasurfaces with a broken-symmetry elements can be engineered to support high-quality (high-Q) resonances associated with the so-called bound states in the continuum, and thus they can demonstrate near-unity CD effects.<sup>8-10</sup>

Nonlinear chiral metadevices require a combination of strong chirality of nonlinear response and high nonlinear conversion efficiency making their development strikingly challenging. For macroscopic nonlinear structures high conversion efficiency is achieved by implying phase matching.<sup>11</sup> Metasurfaces are free from the phase matching constraints because of subwavelength spatial dimensions, and thus their nonlinear response is governed mainly by resonant properties of the structure and the mode overlap. Dielectric metasurfaces sustaining electric and magnetic Mie resonances were recently suggested as a promising alternative to nonlinear plasmonic nanostructures for improving the intensity of the nonlinear signal.<sup>12,13</sup> Recently, it was demonstrated that dielectric nanoparticle dimers made of AlGaAs provide high CD of the second-harmonic signal due to excitation of Mie resonances.<sup>14</sup> Also, it was predicted that nonlinear dielectric metasurfaces with asymmetric meta-atoms can be employed to enhance the nonlinear CD up to near-unity values by excitation of bound states in the continuum with high Q factors.<sup>15</sup>

Here, we propose a design of a chiral nonlinear dielectric metasurface supporting high-Q resonant Mie modes in the near-IR. We engineer a silicon metasurface with chiral asymmetric L-shaped meta-atoms and measure its linear and nonlinear spectral response. More specifically, we measure the transmission spectra selectively for left- and right-polarized pump and show experimentally the enhancement of linear chirality in the vicinity of Mie resonances. Next, we demonstrate experimentally large enhancement of nonlinear CD of third-harmonic (TH) response at the resonance with a high-order electric dipole (ED) mode with  $Q$  factor of about 50. We measure the evolution of the nonlinear CD at the resonance depending on the asymmetry parameter  $\alpha$  of the meta-atom, and reveal that it gradually changes from large positive values for negative  $\alpha$  to large negative values for positive  $\alpha$ . We demonstrate experimentally that TH-CD can reach the value of 0.5 at the wavelength of the maximal conversion efficiency.

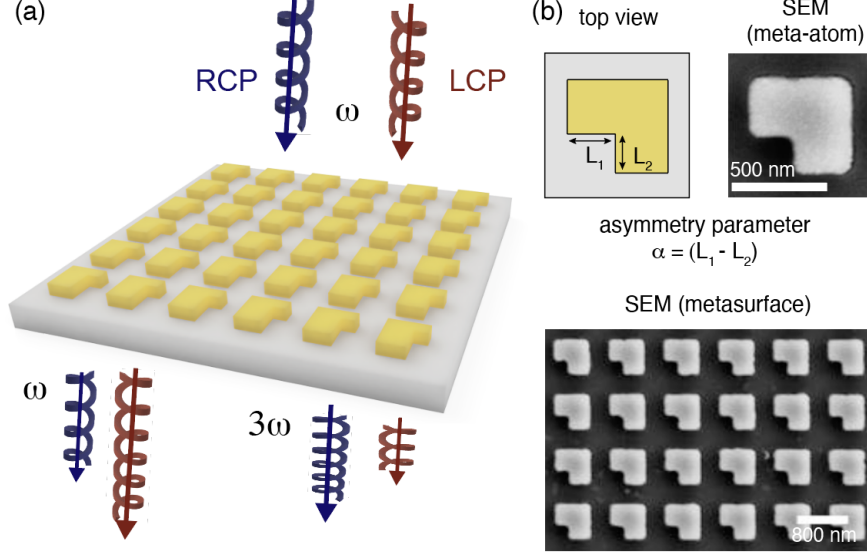


Figure 1: (a) Schematic of a nonlinear chiral resonant metasurface with a broken-symmetry L-shaped meta-atoms. (b) Top: design of a meta-atom and its SEM image. Definition of asymmetry parameter  $\alpha$ . Bottom: SEM image of the metasurface.

## Results and Discussion

Our metasurface consists of an array silicon L-shaped bars on top of a fused silica substrate arranged in a set of asymmetric square unit cells with a period of 840 nm, as shown in Fig. 1(a). The characteristic dimensions of meta-atoms are 525 by 315 nm, the asymmetry parameter  $\alpha$  is defined as the difference  $L_1 - L_2$ , where  $L_2$  is 210 nm and  $L_1$  takes values from 100 to 300 nm [see Fig. 1(b), upper panel]. We engineer the metasurface to support several Mie modes in the near-infrared spectral range with radiative quality (Q) factors from a few tens to a few thousand. We fabricate a set of samples with the parameter  $L_1$  changing from 100 to 300 nm with a step of 10 nm. An example of meta-atom and metasurface scanning electron microscope (SEM) image is shown in Fig. 1(b).

To study the chiroptical response, we first calculate the transmission intensity  $I_{\text{RCP}}^{(\omega)}$  and  $I_{\text{LCP}}^{(\omega)}$ . Each intensity is evaluated for selective circularly-polarized excitation and selective collection of the same polarization at the output, i.e. LCP-to-LCP and RCP-to-RCP transmission without polarization conversion. More details on simulation procedure can be found in Methods. For simulations we select the metasurface with nonzero but small asymme-

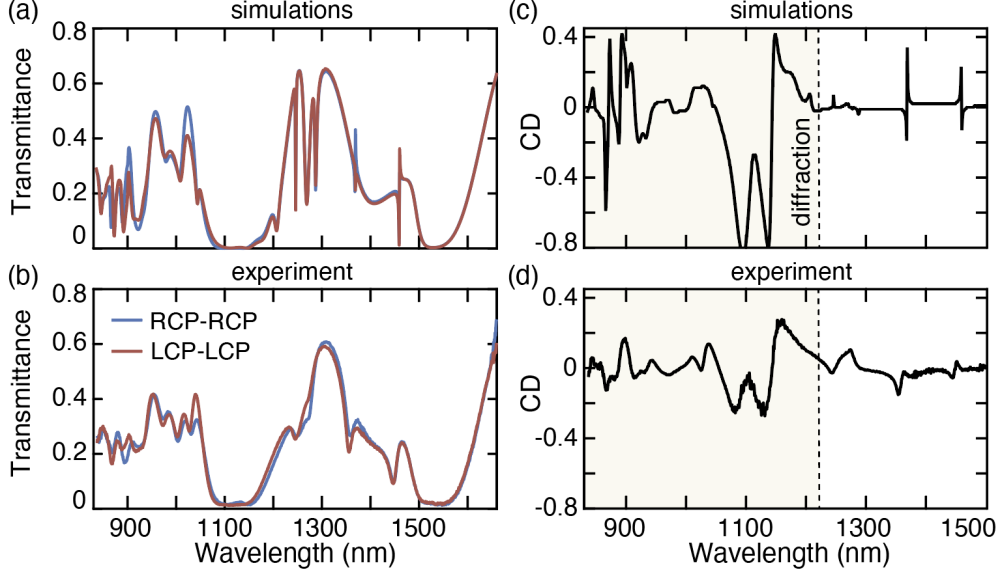


Figure 2: (a,b) Simulated (a) and measured (b) transmittance spectra for selective LCP-LCP (red) and RCP-RCP (blue) excitation and collection. (c,d) Simulated (c) and measured (d) spectrum of linear CD in transmission. The wavelengths below the first diffraction limit are shown with a yellow shaded area. Numerical calculations in (a,b) and experimental data in (c,d) are presented for  $\alpha = 20$  nm.

try parameter,  $\alpha = 20$  nm, because for  $\alpha = 0$  the structure is non-chiral due to in-plane mirror-reflection symmetry of the meta-atom.<sup>8</sup> The linear CD  $\eta^{(\omega)}$  is calculated as

$$\eta^{(\omega)} = \frac{I_{\text{RCP}}^{(\omega)} - I_{\text{LCP}}^{(\omega)}}{I_{\text{RCP}}^{(\omega)} + I_{\text{LCP}}^{(\omega)}}. \quad (1)$$

We note that such method of calculation is consistent with the reciprocity and energy conservation identities and gives  $\eta^{(\omega)} = 0$  for achiral structures unlike the definitions accounting for the cross-polarized transmitted signals.<sup>8</sup>

The simulated transmittance and linear CD for  $\alpha = 20$  nm is shown in Fig. 2(a,c), respectively. The transmission spectra show Fano-type spectral features that correspond to excitation of Mie resonances in the metasurface. For the wavelengths in the vicinity of the first-order diffraction order (about 1220 nm) the Rayleigh anomalies contribute the transmittance. Symmetry requirements impose that the linear CD in the designed structure is driven by interaction of modes with the substrate and diffraction.<sup>10</sup> The CD shows asymmetric

resonant features in the vicinity of peculiarities of transmission spectra reaching the values of about 0.3 in the sub-diffractive regime. In the wavelength range beyond the first-order diffraction limit, shown with a yellow shaded area in Fig. 2(c), the CD increases to very large values, but practically this case is not of high interest because sufficient amount of energy is transferred to diffracted waves.

As the next step, we measure the transmission intensity and linear chirality for selective LCP and RCP excitation and collection. In the linear optical measurement, the circularly polarized white light from a halogen lamp is focused onto the metasurface by an objective lens with NA of 0.25. After passing through the dielectric metasurface, the transmitted light is collected by another objective lens with the same NA. The transmission spectra of the transmitted light with LCP and RCP components are further analyzed with a near-infrared spectrometer (see Methods for details). The measured spectra are shown in Fig. 2(b,d) for the transmittance and CD, respectively. We observe a good agreement between the measurements and simulations. In more detail, the position of resonant features in the experimental data coincides well with the numerical results, while the measured linewidths are larger than in simulations. This can be explained by fabrication imperfections clearly visible in the SEM image (see Fig. 1b) which usually lead to decrease of the Q factor due to parasitic surface scattering.<sup>16</sup> From the measured transmittance we estimate that the total Q factor of the resonant modes is limited by 100.

We simulate third-harmonic generation for the designed silicon metasurface with  $\alpha = 20$  nm and calculate its chiral nonlinear response. The TH signal is evaluated in the undepleted pump approximation valid in the assumption of low input power. More details on nonlinear simulations can be found in Methods. The strength of the TH signal is proportional to the third power of the resonant field enhancement which is determined by the ratio between the radiative and total quality factors.<sup>17</sup> The highest conversion efficiency can be achieved at the so-called optimal coupling regime when the rates of radiative and all other mode losses are equal.<sup>18</sup> For our sample the estimated total Q factor is limited by 100. So

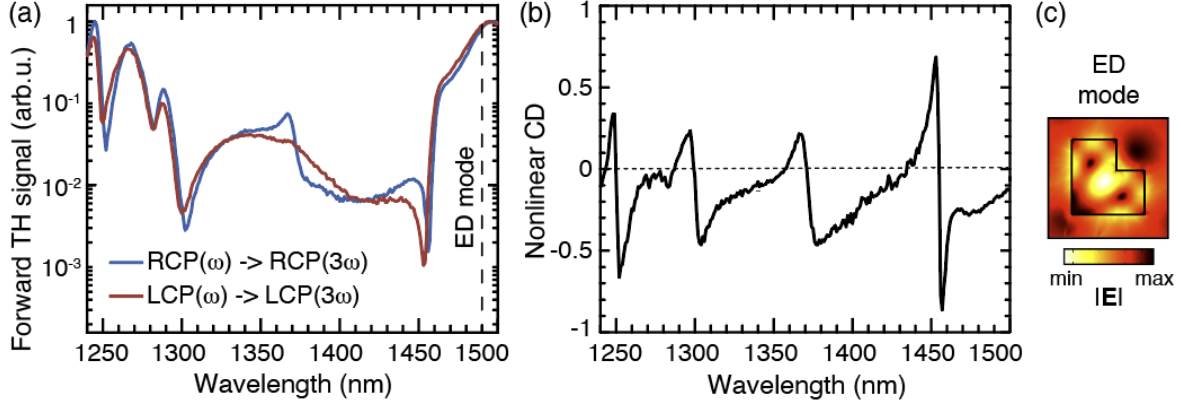


Figure 3: (a) Simulated spectra of forward TH signal for selective LCP-LCP (red) and RCP-RCP (blue) excitation (at  $\omega$ ) and collection (at  $3\omega$ ). The wavelength of the ED mode is marked with a dashed line. (b) Simulated spectrum of nonlinear CD for the TH signal. The dotted line shows the zero level. The calculations in (a,b) are done for  $\alpha = 20$  nm. (c) Electric field profile for the ED mode.

we expect that excitation of the modes with a Q factor much higher or much lower than 100, in particular, very high-Q states that were associated with sharp features in the linear spectra (see Fig. 2), will give a weak nonlinear TH signal. We also expect the modes with a moderate Q factor of order 50 to 200 to provide the highest conversion efficiency and focus on the nonlinear CD behaviour in the vicinity of their wavelengths.

We calculate the intensities of forward scattered TH signal  $I_{\text{RCP}}^{(3\omega)}$  and  $I_{\text{LCP}}^{(3\omega)}$  for right- and left-polarized pump and harmonic, respectively. We note that we consider the normally diffracted harmonic signal only. We take into account the fabrication imperfections associated with surface roughness and parasitic Q factor of 100 by introducing manually artificial absorption for Si, for more details see Methods. As for the linear case, each intensity is evaluated for selective circularly-polarized excitation and selective collection of harmonic with the same polarization at the output. The nonlinear CD for the TH signal  $\eta^{(3\omega)}$  is defined in a similar manner to the linear CD

$$\eta^{(3\omega)} = \frac{I_{\text{RCP}}^{(3\omega)} - I_{\text{LCP}}^{(3\omega)}}{I_{\text{RCP}}^{(3\omega)} + I_{\text{LCP}}^{(3\omega)}}. \quad (2)$$

We notice that in the literature the definition of nonlinear CD is ambiguous, and we select the

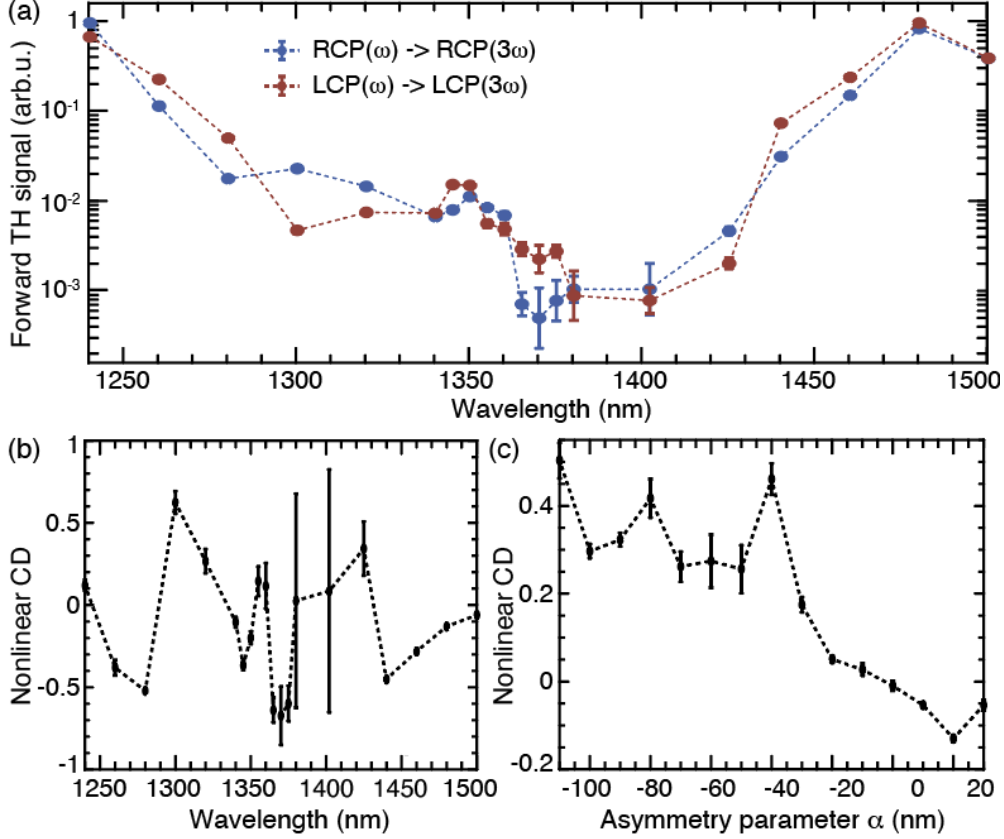


Figure 4: (a) Measured spectra of forward TH signal for selective LCP-LCP (red) and RPC-RCP (blue) excitation (at  $\omega$ ) and collection (at  $3\omega$ ). The maximal signal is achieved in the vicinity of the wavelength of the ED mode. (b) Measured spectrum of nonlinear CD for the TH signal. The measurements in (a,b) are done for the sample with  $\alpha = 20$  nm. (c) Measured nonlinear CD in the vicinity of the wavelength of the ED mode for samples with different  $\alpha$ .

definition that does not include the terms describing polarization conversion. The calculated forward TH signal and nonlinear CD for the sample with  $\alpha = 20$  nm is shown in Fig. 3(a,b), respectively. The spectrum of TH CD shows strong maxima with asymmetric features in the vicinity of high-Q Mie modes but as it was expected the value of conversion efficiency for both polarizations is low at these wavelengths. The highest conversion efficiency is achieved around the high-order electric dipole (ED) mode resonant at 1500 nm with Q factor of 50, which field profile is shown in Fig. 3(c).

Following the nonlinear simulation results, we measure the TH chiral response of the metasurface with  $\alpha = 20$  nm, shown in Fig. 4(a,b). For nonlinear measurements we use a

spectrally tunable femtosecond laser to excite the metasurface and collect the TH signals in the transmission direction with a spectrometer equipped with an EMCCD detector (see Methods for details). The highest conversion efficiency is achieved at the wavelength of 1480 nm. This coincides well the simulation results so we expect that the high-order ED mode in the fabricated sample is resonant at about 1480–1500 nm. The measured nonlinear CD spectrum in Fig. 4(b) demonstrates a sufficient error for the wavelengths in the range 1350 to 1450 nm due to low absolute value of the harmonic signal. To understand what maximal value of TH-CD we can achieve keeping the nonlinear signal high we measure the nonlinear chiroptical response for engineered metasurfaces with different  $\alpha$  from  $-110$  nm to  $30$  nm. We take one measurement for each sample at the wavelength of the ED mode where the TH signal is the strongest, the experimental data is shown in Fig. 4(c). One can see that asymmetry of the meta-atom provides a way to control the nonlinear CD which exhibits a drastic change from  $0.5$  at  $\alpha = -110$  nm to  $-0.13$  at  $\alpha = 20$  nm. We note that due to the specific definition of  $\eta^{(3\omega)}$  we used in Eq. 2 the TH CD is zero for  $\alpha = 0$ , for which the structure linear response becomes achiral.

## Conclusions

We have engineered a chiral silicon metasurface with L-shaped meta-atoms for enhanced nonlinear chiroptical response. We have simulated numerically and measured experimentally transmission spectra selectively for left- and right-polarized pump and showed experimentally the increase of linear chirality in the vicinity of Mie resonances. We have noticed that linear CD is determined by the mode interaction with a substrate and diffraction at short wavelengths. We have demonstrated numerically and experimentally large enhancement of nonlinear CD for third-harmonic (TH) response at wavelength of the highest nonlinear conversion efficiency for samples with different asymmetry of the unit cell. We have shown that the highest TH signal is achieved at the resonance with a high-order electric dipole

mode with the  $Q$  factor of 50 which satisfies the optimal coupling condition of maximal local field enhancement. We have demonstrated experimentally that TH-CD can reach the value of 0.5 at the wavelength of maximal conversion efficiency.

## Materials and Methods

**Sample fabrication.** The metasurfaces composed of silicon L-shaped meta-atoms were plasma etched from a 315 micron thick  $\alpha$ -Si layer deposited by LPCVD process on an RCA cleaned fused silica wafer. The metasurface was delineated first by electron beam lithography process conducted by means of JEOL 9300FS 100kV system in PMMA 950k electron beam resist, 200 nm thick. A 5 nm thin Cr-metal film vacuum evaporated onto PMMA coated wafer surface was utilized as a charge dissipation layer during the e-beam exposure process. Before developing the exposed resist in an MIBK/IPA developer, this metal film was removed by a standard Cr-metal etchant followed by DI water rinse. A 10 nm thin Cr-metal hard mask for the plasma etch process was then created by the lift-off procedure during sonication of the wafer in acetone out of a second vacuum evaporated Cr metal film on the developed resist surface. This mask was also removed by the wet chemical etch process after the plasma etch process was completed before commencing the optical measurements.

**Optical measurements.** For the linear optical measurements, the circular polarization states of the white light from a halogen lamp are prepared using a linear polarizer (LP) and a subsequent achromatic quarter-wave plate (QWP). The white light is focused onto the metasurface and collected in the transmission direction using a pair of objective lenses (NA = 0.25). After selectively filtering out the LCP and RCP polarization components, the transmitted light is spectrally resolved by using a near-infrared spectrometer (Andor-328i). In the nonlinear optical measurements, we use a femtosecond laser pumped optical parametric oscillator (repetition frequency: 80 MHz, pulse duration: 250 fs). The central wavelength of the pumping laser is tuned from 1240 nm to 1500 nm. After passing through

a LP and a QWP, the circularly polarized laser is focused onto the metasurface from the air side using an objective lens (NA = 0.1), the spot size was about 20  $\mu\text{m}$  in diameter. The TH signals with LCP and RCP polarization components are collected in the transmission direction by another objective lens (NA = 0.25) and then spectrally resolved through an Andor spectrometer (SP500i) equipped with an EMCCD detector.

**Numerical simulations.** For numerical simulations of the transmission spectrum, we use the finite-element-method solver in COMSOL Multiphysics in the frequency domain. The near-field distributions are simulated using the eigenmode solver in COMSOL Multiphysics. All calculations were realized for a metasurface placed on a semi-infinite substrate surrounded by a perfectly matched layer mimicking an infinite region. The simulation area is the unit cell extended to an infinite metasurface by using the Bloch boundary conditions. The material properties, including absorption losses, are extracted from the ellipsometry data for Si and imported from the tabulated data for a fused silica substrate. The incident field is a plane wave in the normal excitation geometry with left or right circular polarization. The nonlinear simulations of TH response are employed within the undepleted pump approximation, using two steps to calculate the intensity of the radiated nonlinear signal. First, we simulated the linear scattering at the pump wavelength, and then obtained the nonlinear polarization induced inside the meta-atom. Then, we employed the polarization as a source for the electromagnetic simulation at the harmonic wavelength to obtain the generated TH field. The nonlinear susceptibility function  $\chi^{(3)}$  was considered as a tensor corresponding to the cubic crystallographic point group with  $\chi_{xxxx}^{(3)} = 2.45 \times 10^{-19} \text{ m}^2/\text{V}^2$ . For nonlinear simulations we take into account the parasitic losses due to surface roughness which are introduced artificially by adding of artificial extinction  $k = n/(2Q_{\text{par}})$ , where  $n$  is the refractive index and  $Q_{\text{par}} = 100$  is the Q factor describing parasitic losses extracted from the linear transmittance data.

## Acknowledgement

The authors acknowledge useful comments and suggestions received from Maxim Gorkunov. The work was financially supported by the Australian Research Council (grants DP200101168 and DP210101292), the Russian Science Foundation (18-72-10140), and Priority 2030 Federal Academic Leadership Program.

## References

- (1) Valev, V. K.; Baumberg, J. J.; Sibilica, C.; Verbiest, T. Chirality and chiroptical effects in plasmonic nanostructures: fundamentals, recent progress, and outlook. *Advanced Materials* **2013**, *25*, 2517–2534.
- (2) Ren, M.; Plum, E.; Xu, J.; Zheludev, N. I. Giant nonlinear optical activity in a plasmonic metamaterial. *Nature communications* **2012**, *3*, 1–6.
- (3) Solomon, M. L.; Hu, J.; Lawrence, M.; García-Etxarri, A.; Dionne, J. A. Enantiospecific optical enhancement of chiral sensing and separation with dielectric metasurfaces. *ACS Photonics* **2018**, *6*, 43–49.
- (4) Ma, Z.; Li, Y.; Li, Y.; Gong, Y.; Maier, S. A.; Hong, M. All-dielectric planar chiral metasurface with gradient geometric phase. *Optics Express* **2018**, *26*, 6067–6078.
- (5) Tang, Y.; Liu, Z.; Deng, J.; Li, K.; Li, J.; Li, G. Nano-Kirigami metasurface with giant nonlinear optical circular dichroism. *Laser & Photonics Reviews* **2020**, *14*, 2000085.
- (6) Tanaka, K.; Arslan, D.; Fasold, S.; Steinert, M.; Sautter, J.; Falkner, M.; Pertsch, T.; Decker, M.; Staude, I. Chiral bilayer all-dielectric metasurfaces. *ACS nano* **2020**, *14*, 15926–15935.
- (7) Ye, W.; Yuan, X.; Guo, C.; Zhang, J.; Yang, B.; Zhang, S. Large chiroptical effects in planar chiral metamaterials. *Physical Review Applied* **2017**, *7*, 054003.

- (8) Gorkunov, M. V.; Antonov, A. A.; Kivshar, Y. S. Metasurfaces with maximum chirality empowered by bound states in the continuum. *Physical Review Letters* **2020**, *125*, 093903.
- (9) Overvig, A.; Yu, N.; Alù, A. Chiral quasi-bound states in the continuum. *Physical Review Letters* **2021**, *126*, 073001.
- (10) Gorkunov, M. V.; Antonov, A. A.; Tuz, V. R.; Kupriianov, A. S.; Kivshar, Y. S. Bound States in the Continuum Underpin Near-Lossless Maximum Chirality in Dielectric Metasurfaces. *Advanced Optical Materials* **2021**, *9*, 2100797.
- (11) Armstrong, J.; Bloembergen, N.; Ducuing, J.; Pershan, P. S. Interactions between light waves in a nonlinear dielectric. *Physical review* **1962**, *127*, 1918.
- (12) Kuznetsov, A. I.; Miroshnichenko, A. E.; Brongersma, M. L.; Kivshar, Y. S.; Luk'yanchuk, B. Optically resonant dielectric nanostructures. *Science* **2016**, *354*, aag2472.
- (13) Koshelev, K.; Kivshar, Y. Dielectric resonant metaphotonics. *Acs Photonics* **2020**, *8*, 102–112.
- (14) Frizyuk, K.; Melik-Gaykazyan, E.; Choi, J.-H.; Petrov, M. I.; Park, H.-G.; Kivshar, Y. Nonlinear circular dichroism in Mie-resonant nanoparticle dimers. *Nano Letters* **2021**, *21*, 4381–4387.
- (15) Gandolfi, M.; Tognazzi, A.; Rocco, D.; De Angelis, C.; Carletti, L. Near-unity third-harmonic circular dichroism driven by a quasibound state in the continuum in asymmetric silicon metasurfaces. *Physical Review A* **2021**, *104*, 023524.
- (16) Kühne, J.; Wang, J.; Weber, T.; Kühner, L.; Maier, S. A.; Tittl, A. Fabrication robustness in BIC metasurfaces. *Nanophotonics* **2021**, *10*, 4305–4312.

- (17) Koshelev, K.; Tang, Y.; Li, K.; Choi, D.-Y.; Li, G.; Kivshar, Y. Nonlinear metasurfaces governed by bound states in the continuum. *ACS Photonics* **2019**, *6*, 1639–1644.
- (18) Bernhardt, N.; Koshelev, K.; White, S. J.; Meng, K. W. C.; Froch, J. E.; Kim, S.; Tran, T. T.; Choi, D.-Y.; Kivshar, Y.; Solntsev, A. S. Quasi-BIC resonant enhancement of second-harmonic generation in WS<sub>2</sub> monolayers. *Nano Letters* **2020**, *20*, 5309–5314.